Available online at www.sciencedirect.com

SciVerse ScienceDirect

Energy Procedia 37 (2013) 1067 – 1075

Energy Procedia

GHGT-11

PAMAM dendrimer containing polymeric membrane for preferential CO_2 separation over H_2 - Interplay between CO_2 separation properties and morphology

Ikuo Taniguchi,[a,]* Teruhiko Kai,[a] Shuhong Duan,[a] and Shingo Kazama[b]

[a]*Chemical Research Group, Research Institute of Innovative Technology for the Earth, 9-2 Kizugawadai, Kizugawa, Kyoto 619-0292, Japan*

[b]*Technical Development Bureau, Nippon Steel Corporation, 2-6-1 Marunouchi, Chiyoda-ku, Tokyo, 100-8071, Japan*

Abstract

Poly(amidoamine) (PAMAM) dendrimer is entrapped in a poly(ethylene glycol) network by photo-polymerization of PEG dimethacrylate (PEGDMA) in the presence of the dendrimer. The resulting polymeric membrane displays excellent CO_2 separation properties over H_2. The dendrimer content, generation of the dendrimer, and relative humidity are crucial factors to characterize CO_2 separation performance of the dendrimer containing polymeric membrane. Especially, the UV curing of immiscible pair of the dendrimer and PEG results in the formation of a bicontinuous structure upon macrophase separation in a coupe of microns scale. The phase-separated structure also determines preferential CO_2 permeation.

Selection and/or peer-review under responsibility of GHGT

Keywords: CO_2 separation; Phase separation; Poly(amidoamine) dendrimer; Poly(ethylene glycol); Polymeric membrane

1. Introduction

Recent intensive investigations have warned against global climate change and global warming triggered by the rise in atmospheric concentration of greenhouse gases, particularly CO_2. After the Fukushima disaster in 2011, Japan is facing to reduce the dependence on nuclear power and the ratio of electric power generation by coal-fired power plant has been raised. Mitigation of CO_2 emission has been

* Corresponding author. Tel.: +81-774-75-2305; fax: +81-774-75-2318.
E-mail address: taniguti@rite.or.jp.

1876-6102
Selection and/or peer-review under responsibility of GHGT
doi:10.1016/j.egypro.2013.05.203

thus an urgent matter. CO_2 capture and storage (CCS) can be a promising candidate toward global warming and have been studied extensively [1]. In CCS, CO_2 capturing or separation dominates about 60 % of the total cost, and cost reduction of CO_2 separation is the key issue for implementation of CCS.

Various CO_2 separation technologies have been investigated [1-3], and solvent absorption such as Selexol has gained current acceptance [4,5]. However, regeneration of CO_2 requires heating of the CO_2 containing solution after CO_2 absorption, which results in considerable energy consumption. On the other hand, difference in partial pressure of an interested gas between feed and permeate side can be a driving force in membrane separation, and when the feed gas has pressure, additional energy such as heating is not required. In addition, the infrastructure of membrane modules can be much smaller in comparison to that of the solvent absorption. Membrane separation is thus expected as a next generation technology [6-8]. Our current target is CO_2 separation over H_2 for use such as in an integrated gasification combined cycle plant with CCS. Here, H_2 is smaller than CO_2 so that the CO_2 separation does not proceed by conventional molecular sieving mechanism.

In this research group, PAMAM dendrimers have been used as a CO_2-specific agent [9-11]. The dendrimers are the first successfully developed and one of the most investigated dendritic structures [12]. Potential applications of the dendrimers have been investigated, including biomedical and pharmaceutical uses [13,14]. Besides the versatile potentials, another fascinating feature of PAMAM dendrimer was first reported by Sirker and coworkers. The dendrimer exhibited preferential permeation of CO_2 over a gas mixture with a liquid immobilized membrane system [15]. However, the dendrimers flows at ambient conditions, which limits use under pressure. Recently, effective immobilization of the dendritic molecules in a PEG network was reported by photo-polymerization of PEGDMA in the presence of the dendrimer as shown in Fig. 1 [16]. A self-standing polymeric membrane is fabricated when the dendrimer concentration is below 70 wt%. The resulting polymeric membrane exhibits excellent CO_2 separation properties depending on the dendrimer content, generation of the dendrimer, humidity, and phase-separated structure [16-18]. Interplay between CO_2 separation performance and the morphology is investigated.

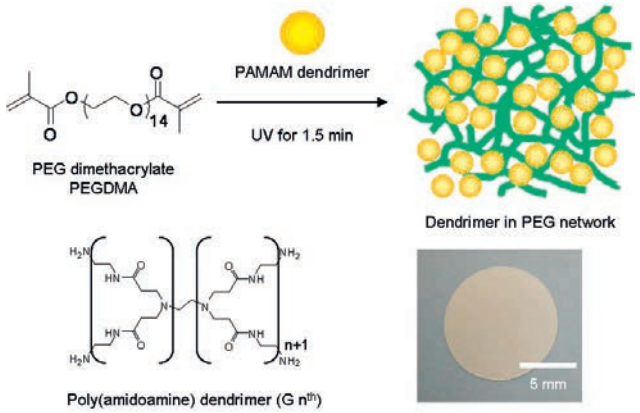

Fig. 1. Schematic drawing of membrane fabrication and the resulting polymeric membrane

2. Experimental

2.1. Materials

PEGDMAs with various PEG length (EG unit: 3 (286 in FW), 9 (550), and 14 (550)), PAMAM dendrimers in methanol solution, and 1-hydroxycyclohexyl phenylketone (HCPK) were obtained from Aldrich (WI). PEGDMA with EG unit 23 and FITC-bearing PEGMA were synthesized in the previous work [17]. Other organic and inorganic materials were reagent grade and used without further purification.

2.2. Membrane fabrication

Membrane preparation was basically the same as described in the previous report [16]. Briefly, PAMAM dendrimer (2.0 g, 3.9 mmol) and PEGDMA (2.0 g, 2.7 mmol) were dissolved in ethanol (2.0 g) containing HCPK (9.1 mg, 44 μmol) under shading, where methacrylate to initiator ratio was 60 by the molar ratio. The reaction mixture was cast into a Teflon dish (ID: 60 mm) and exposed to UV light (365 nm, 12 mW/cm^2) (UVP B-100AP, CA, USA) for 90 s at ambient temperature to photo-crosslink PEGDMA. After dried under vacuum, a polymeric membrane with 50 wt% PAMAM dendrimer was obtained, and the thickness was ca. 500 μm. FITC-labeled polymeric membrane was prepared by copolymerization of PEGDMA with FITC-PEGMA [17].

2.3. LSCM observation

Phase-separated structure of the polymeric membrane was observed on a laser scanning confocal microscope (LSCM). The phase-separated structures of the polymeric membranes were measured by a LSM 710 (Carl Zeiss, Germany) with an incident laser beam (488 nm). A band-pass filter (490-735 nm) installed in front of the detector was used to detect only fluorescence from the fluorescent molecules that were introduced only to stain the PEG-rich phase. The PEG network was thus recognized as a bright phase under fluorescent LSCM. An oil-immersed ×63 (Plan-Apochromat, Carl Zeiss) objective lens with numerical aperture of 1.4 was used. Fluorescence images sliced at intervals of 434 nm in depth were collected, which were processed to reconstruct a 3D structure. Only PEG-rich phase stained with FITC was seen in this experimental setup.

2.4. Gas separation test

CO_2 separation properties over H_2 of the polymeric membrane were measured at 298 K under atmospheric pressure. The surface area of the membrane was 8.04 cm^2. A CO_2/H_2 gas with 5 vol% of CO_2 was humidified at various humidity and 298 K, and fed at a flow rate of 100 mL/min. Helium was supplied to the permeate side of the cell as a sweep gas at a flow rate of 10 mL/min. Composition of the permeate was analyzed on a GC4000 gas chromatograph with a pulsed discharge detector (GL Science, Tokyo, Japan), while the feed side was with a thermal conductivity detector (GL Science). Permeance of gas *i* (Q_i) and separation factor ($\alpha_{CO2/H2}$) were determined by the following equations (Eqs. 1 and 2), where N_i, A, Δp, and t were permeate gas volume of gas *i*, membrane area, partial pressure difference of the feed and permeate gas, transmission time, respectively. In Eq. 2, x_i, and y_i denoted molar fraction of gas *i* of feed and permeate sides, respectively.

$$Q_i = N_i/(A\ \Delta p\ t) \tag{1}$$

$$\alpha_{CO2/H2} = (y_{CO2}/y_{H2})/(x_{CO2}/x_{H2}) \tag{2}$$

3. Results and discussion

PAMAM dendrimer and PEGDMA are immiscible, and in the membrane fabrication, ethanol was used to obtain homogeneous mixture. Polymeric membranes composed of PAMAM dendrimer in a crosslinked PEG were successfully obtained by UV curing of PEGDMA in the presence of the dendrimer and were self-standing with PAMAM content below 70 wt%. The polymeric membranes became opaque by inclusion of the dendrimer, which would be due to phase separation in a couple of microns scale. Hereafter, PAMAM dendrimer with generation 0 was used.

3.1. Determination of macrophase-separated structure

The detailed morphology was examined with LSCM by staining only polymer matrix with FITC. The raw image was presented in Fig. 2a, where dark field represented the dendrimer-rich phase, while bright phase the PEG-rich phase. The interface of the co-existing phase was extracted by image processing, such as contrast variance enhancement method and median filter treatment [17,19]. The 3D structure was reconstructed by stacking the processed images at each depth with an IMARIS software (Bitplane, Germany) in Fig. 2b [17,19]. Macrophase separation was clearly seen, and immiscible pair of PAMAM and PEG resulted in the formation of a bicontinuous structure. The result suggested that the dendrimer-rich phase penetrated through the polymeric membrane, where CO_2 would permeate.

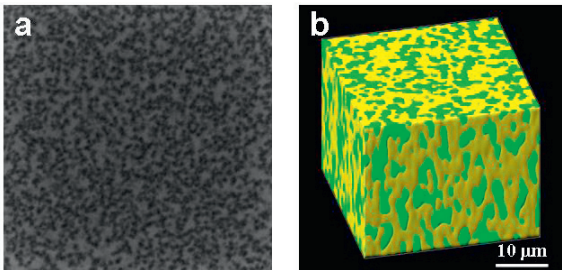

Fig. 2. Phase-separated structure of PAMAM dendrimer (50 wt%) in PEG network by LSCM. (a) raw image at 50 μm depth (45 × 45 μm) and (b) reconstructed 3D structure (green: PEG-rich phase, yellow: PAMAM-rich phase, 35 × 35 × 30 μm)

Fourier-transformation of the summed images at each depth was conducted. A plot of the magnitude of the Fourier transformation as a function of the wavenumber (q) gave a peak originated from a periodical structure of the PEG-rich phase as described in Fig. 3. The average PAMAM domain size (Λ_m) was calculated from the q at the peak top (q_m) by Eq. 3. The results were summarized in Table 1.

$$\Lambda_m = 2\pi/q_m \quad (3)$$

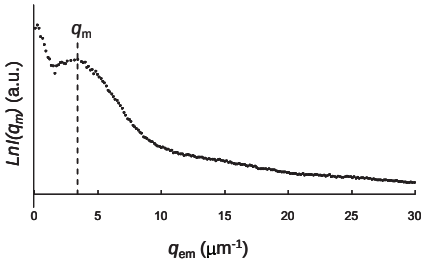

Fig. 3. A plot of the magnitude of the Fourier transformation as a function of the wavenumber (PAMAM content: 30 wt%)

Table 1. Effect of PAMAM dendrimer concentration and PEG length on macrophase separation

[PAMAM]/wt%	PAMAM/vol%	Average EG unit	Average PAMAM domain size/μm
30	44.3 ± 0.2	14	2.0 ± 0.1
50	49.2 ± 1.0	14	2.2 ± 0.2
70	56.0 ± 0.3	14	4.1 ± 0.0
50	47.5 ± 2.4	3	2.8 ± 0.1
50	49.9 ± 2.0	9	2.6 ± 0.2
50	50.9 ± 0.5	23	2.7 ± 0.1

± denotes standard deviation (n = at least 3).

The PAMAM volume fraction and the average PAMAM domain size increased with increase in PAMAM concentration in the polymeric membrane when the average EG unit was 14. The PAMAM volume fraction did not match with the concentration, which would be due to partial mixing. On the other hand, the PAMAM domain size was depended on the PEG length (EG unit) and polymeric membrane with EG unit of 14 gave the smallest domain size, or the highest degree of phase separation, when PAMAM content was fixed to 50 wt%.

3.2. CO_2 separation properties

CO_2 separation properties of the polymeric membranes were examined, and effect of PAMAM dendrimer concentration and generation of the dendrimer were represented in Fig. 4. Permeability P can be given by $P = Q \times l$, where l is membrane thickness. Permeability of CO_2 increased slightly while that of H_2 decreased significantly with increase in PAMAM concentration. As a result, the polymeric membrane exhibited excellent CO_2 separation selectivity. When PAMAM concentration was 50 wt%, $\alpha_{CO2/H2}$ reached about 500. This result implies that PAMAM dendrimer inhibits permeation of H_2 by so-called "*CO_2-selective Molecular Gate*" effect proposed by Sirkar and coworkers rather than enhancing CO_2 permeation [15]. Due to the specific interaction between CO_2 and primary amine of the dendrimer,

the solubility of CO_2 was much higher than H_2, and the free volume of the polymeric membrane was mostly occupied with CO_2. As a consequence, permeation of H_2 was considerably suppressed.

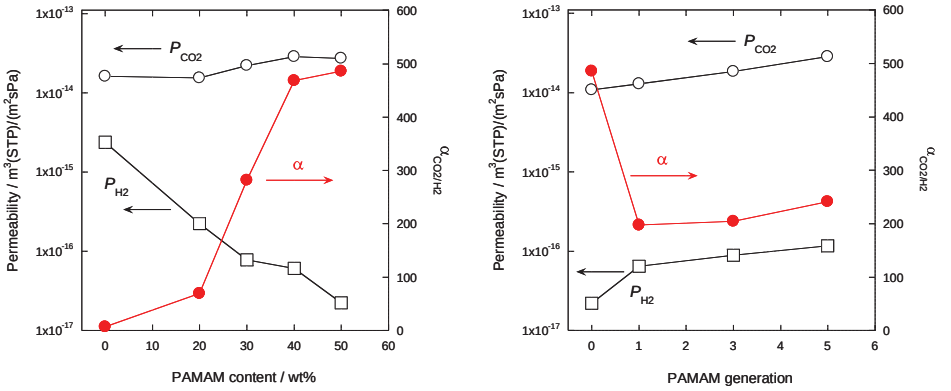

Fig. 4. Effect of PAMAM concentration (a) and of the dendrimer generation when PAMAM was 50 wt% (b) on CO_2 separation properties of PAMAM dendrimer containing membrane at 298 K and 80 % relative humidity (p_{CO2} = 5 kPa) [16]

On the other hand, polymeric membranes with various dendrimer generations were prepared, in which the dendrimer content was kept 50 wt%. Both of permeabilities rose with increase of the dendrimer generation. Higher generation dendrimer should have higher void volume in the interior core, where smaller H_2 penetrates much readily. The smallest 0^{th} generation dendrimer gave the highest CO_2 separation factor over H_2. The gas separation test was conducted under relative humidity of 80 % because in practical condition, such as in IGCC, after water-gas shit reaction, the synthesis gas is saturated with water vapor. Membranes, which work under humidified condition, are thus sought after.

The polymeric membranes are turbid after evaporation of ethanol and turn to transparent under humidified condition. LSCM observation suggests phase mixing by absorbing water, and the interface becomes ambiguous. CO_2 separation properties of the polymeric membrane (EG unit: 14, PAMAM: 50 wt%) are strongly depended on humidity as shown in Table 2. The Q_{CO2} increased with increase in the relative humidity from 3.96×10^{-13} to 1.38×10^{-11} $m^3(STP)/(m^2\ s\ Pa)$ while the Q_{H2} did not change much over the humidity examined. As a result, higher relative humidity resulted in higher separation factor. Upon humidification, the absorbed water can be a compatibilzer, which facilitates the dendrimer diffusion into PEG-rich phase. The membrane can be homogeneous under humidified conditions, which leads to enhance CO_2 sorption, and thus a higher CO_2 permeation is seen at higher relative humidity.

Table 2. Effect of CO_2 separation properties on relative humidity

Relative humidity/%	Q_{CO2}	Q_{H2}	$\alpha_{CO2/H2}$
0	3.96×10^{-13}	9.70×10^{-15}	40.8
30	4.75×10^{-13}	6.71×10^{-15}	70.7
50	1.08×10^{-12}	9.15×10^{-15}	117.9
80	1.38×10^{-11}	2.62×10^{-14}	523.6

The polymeric membrane composed of PEGDMA (EG unit: 14) with 50 wt% PAMAM dendrimer (G: 0). Q: $m^3(STP)/(m^2\ s\ Pa)$

Polymeric membranes with various PEG lengths were fabricated (PAMAM: 50 wt%), and effect of PEG length on the CO_2 separation performance was studied. Gas permeances of the polymeric

membranes were listed in Table 3. Although the deviations were not small, the polymeric membranes with EG 9 and 14 gave higher Q_{CO2} than the others. Fig. 5 describes interplay between CO_2 selectivity over H_2 and PAMAM domain size. Polymeric membranes with EG 9 and 14 express higher CO_2 selectivity. On the other hand, those membranes exhibit smaller PAMAM domain size. The obtained results suggest that smaller dendrimer domain size, or higher degree of phase separation, gives higher CO_2 selectivity. At higher degree of phase separation, the dendrimer can diffuse more homogeneously throughout the polymeric membrane under humidified condition, so that CO_2 permeation would be faster than that with lower degree of phase separation, or larger PAMAM domain size.

Table 3. Effect of PEG length on gas permeance of PAMAM dendrimer containing polymeric membrane

EG length	Q_{CO2}	Q_{H2}
3	$(2.55 \pm 1.50) \times 10^{-12}$	$(1.57 \pm 0.33) \times 10^{-14}$
9	$(1.24 \pm 0.54) \times 10^{-11}$	$(2.71 \pm 0.42) \times 10^{-14}$
14	$(2.44 \pm 2.05) \times 10^{-11}$	$(4.98 \pm 4.01) \times 10^{-14}$
23	$(5.70 \pm 0.96) \times 10^{-13}$	$(7.56 \pm 4.45) \times 10^{-15}$

[PAMAM] = 50 wt%, Q: $m^3(STP)/(m^2\ s\ Pa)$

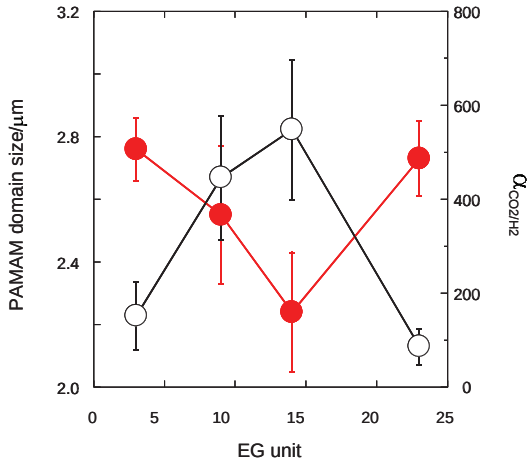

Fig. 5. Interplay between CO_2 selectivity and PAMAM domain size of PAMAM dendrimer containing polymeric membrane with various PEG lengths (PAMAM: 50 wt%)

4. Conclusion

PAMAM dendrimers were successfully and stably immobilized in a PEG network by photo-polymerization of PEGDMA in the presence of the dendrimer. The resulting polymeric membrane showed a bicontinuous structure of PAMAM-rich and PEG-rich phases upon macrophase separation, and the average PAMAM dendrimer domain size was 2-4 microns, depending on PAMAM concentration and PEG length. The polymeric membranes exhibited excellent CO_2 separation properties, which were strongly related to the dendrimer concentration, generation of the dendrimer, humidity, and phase-

separated structure. "*CO_2-selective Molecular Gate*" effect of the dendrimer was suggested. The membrane formulation containing PAMAM dendrimer provides an insight for fabrication of CO_2-specific polymeric materials.

Acknowledgements

This work was financially supported by the Japanese Ministry of Economy, Trade and Industry. The authors wish to acknowledge Mr. Akira Yaguchi for skillful technique on LSCM measurement and Dr. Haruko Saito for analyses of the LSCM results. The authors are also thankful for the assistance of Ms. Hiromi Urai and Rie Sugimoto throughout the membrane fabrication processes and gas chromatography measurements.

References

[1] Wilson E, Gerard D. *Carbon Capture and Sequestration Integration Technology, Monitoring, Regulation*. New York: Wiley; 2007.

[2] Halmann MM, Steinberg M. *Greenhouse Gas Carbon Dioxide Mitigation: Science and Technology*. New York: CRC; 1998.

[3] Metz B, Davidson O, de Coninck H, Loos M, Meyer L. *Carbon Dioxide Capture and Storage: IPCC Special Report of the Intergovernmental Panel on Climate Change*. Cambridge: Cambridge University Press; 2005.

[4] Davis RA, Menendez RE, Sandall OC. Physical, thermodynamic, and transport properties for carbon dioxide and nitrous oxide in solutions of diethanolamine or di-2-propanolamine in polyethylene glycol. *J Chem Eng Data* 1993;38:119-124.

[5] Henni A, Tontiwachwuthikul P, Chakma A, Solubilities of carbon dioxide in polyethylene glycol ethers. *Can J Chem Eng* 2005;83:358-361.

[6] Sirkar KK. Membrane separation technologies: Current developments. *Chem Eng Commun* 1997;157:145-184.

[7] Javaid A. Membranes for solubility-based gas separation applications. *Chem Eng J* 2005;112:219-226.

[8] Chung TS, Jiang LY, Li Y, Kulprathipanja S. Mixed matrix membranes (MMMs) comprising organic polymers with dispersed inorganic fillers for gas separation. *Prog Polym Sci* 2007;32:483-507.

[9] Duan S, Kouketsu T, Kazama S, Yamada K. Development of PAMAM dendrimer composite membranes for CO_2 separation, *J Membr Sci* 2006;283:2-6.

[10] Kouketsu T, Duan S, Kai T, Kazama S, Yamada K. PAMAM dendrimer composite membrane for CO_2 separation: Formation of a chitosan gutter layer. *J Membr Sci* 2007;287:51-59.

[11] Duan S, Taniguchi I, Kai T, Kazama S. Poly(amidoamine) dendrimer/poly(vinyl alcohol) hybridmembranesfor CO_2 capture, *J Membr Sci* in press (DOI: 10.1016/j.memsci.2012.07.037).

[12] Tomalia DA, Baker H, Dewald J, Hall M, Kallos G, Martin S, Roeck J, Ryder J, Smith P. A new class of polymers: Starburst-dendritic macromolecules. *Polym J* 1985;17:117-132.

[13] Rosi NL, Mirkin CA. Nanostructures in biodiagnostics. *Chem Rev* 2005;105:1547-1562.

[14] Lee CC, MacKay JA, Fréchet JMJ, Szoka FC. Designing dendrimers for biological applications. *Nature Biotech* 2005;23:1517-1526.

[15] Kovvali AS, Chen H, Sirkar KK. Dendrimer membranes: a CO_2-selective molecular gate, *J Am Chem Soc* 2000;122:7594-7595.

[16] Taniguchi I, Duan S, Kazama S, Fujioka Y. Facile fabrication of a novel high performance CO_2 separation membrane: immobilization of poly(amidoamine) dendrimers in poly(ethylene glycol) networks. *J Membr Sci* 2008;322:277-280.

[17] Taniguchi I, Kazama S, Jinnai H. Structural analysis of poly(amidoamine) dendrimer immobilized in crosslinked poly(ethylene glycol). *J Polym Sci Part B Polym Phys* 2012;50:1156-1164.

[18] Taniguchi I. Duan S, Kai T, Kazama S, Jinnai H. Poly(amidoamine) Dendrimer Immobilized in a Poly(ethylene glycol) Network: Interplay between Phase-Separated Structure and CO_2 Separation Mechanism. *J Membr Sci* submitted.

[19] Jinnai H, Nishikawa Y, Morimoto H, Koga T, Hashimoto T. Geometrical properties and interface dynamics: Time evolution of spinodal interface in a binary polymer mixture at the critical composition. *Langmuir* 2000;16:4380-4385.